CONCRETE LIBRARY OF JSCE NO. 26, DECEMBER 1995

SIZE EFFECT ANALYSIS FOR SHEAR STRENGTH OF CONCRETE BEAMS BASED ON FRACTURE MECHANICS

(Translation from Journal of Materials, Concrete Structures and Pavements of JSCE, No. 508/V-26, February 1995)



Junichiro NIWA　　Nasra ZAREEN　　Tada-aki TANABE

Diagonal tension failure of concrete beams without web reinforcement is one of the most important issues in concrete mechanics. The size effect in shear strength has been confirmed experimentally. In the JSCE's standard specifications for the design and construction of concrete structures, a design equation which takes into account the size effect is specified. However, with the increasing size of modern concrete structures, the future will see huge concrete structures which exceed the range of applicability of the specifications, and experimental verification will be substantially impossible. In this paper, the size effect on the shear strength of concrete beams is predicted numerically by fracture mechanics.

Key Words: fracture mechanics, shear strength, size effect, finite element analysis, design code

---

Junichiro NIWA is an Associate Professor of Civil Engineering at Nagoya University, Nagoya, Japan. Now he is seconded to Asian Institute of Technology, Bangkok, Thailand. He received his Doctor of Engineering Degree from the University of Tokyo. He specializes in the mechanics of concrete structures including fracture mechanics and nonlinear numerical analysis. He is a member of JSCE, JCI, IABSE, CEB and ACI.

Nasra ZAREEN is presently working as a structural design engineer in Pakistan. She received her Master of Engineering Degree from Nagoya University. Her research interest is related to the size effect in shear strength of concrete beams based on fracture mechanics approach using finite element analysis. She is a member of PEC.

Tada-aki TANABE is a Professor of Civil Engineering at Nagoya University, Nagoya, Japan. He received his Doctor of Engineering Degree from the University of Tokyo. He is the chairman of JCI Committee on the Thermal Stress of Massive Concrete Structures besides a member of various committees of JSCE, JCI, and ACI. His main research is directed to the dynamic failure mechanism of RC structures besides the thermal stress.

1. INTRODUCTION

To predict the resistance to diagonal tension failure of reinforced concrete beams without web reinforcement, numerous experimental investigations have been carried out around the world. Shear failure is completely different from flexural failure, in which a ductile failure mode is exhibited. Shear failure is characterized by a sudden and brittle failure immediately after the propagation of a diagonal crack. This is the reason why it has caught the interest and concern of numerous researchers and engineers. However, it still appears very difficult to deal with shear failure problems purely theoretically.

In 1980, Okamura and Higai proposed the macroscopic shear strength equation [1], that is now known as Okamura and Higai's equation. They proposed this equation based on a qualitative and elaborate consideration of the shear resisting mechanism. Considering a free body of a reinforced concrete beam with a diagonal crack, they divided the shear resisting mechanism just before the shear failure into three components: (1) the aggregate interlocking along the diagonal crack; (2) the dowel action of longitudinal bars; and (3) the direct shear resistance of concrete in the flexural compression zone above the diagonal crack. The remarkable feature of this equation is that the size effect, that is the nominal shear strength is decreasing with increasing beam size, is incorporated.

With demand for large concrete structures growing, Shioya et al. later carried out an experiment on 3-meter-high reinforced concrete beams without web reinforcement and subjected to uniform loading [2]. Furthermore, Yokozawa et al. did experiments on 2-meter-high reinforced concrete beams without web reinforcement and subjected to concentrated loading [3]. Based on these new experimental results, Okamura and Higai's equation was updated to incorporate the size effect more directly [3]. This revised equation is the basis for the design equation stipulated in the current JSCE Standard Specifications.

In the ACI Building Code Requirements (ACI 318), no attention is paid to the size effect in shear strength even in the 1989 version [4]. On the other hand, the CEB-FIP Model Codes, both in 1978 and in 1990, consider the size effect in shear strength very clearly [5][6].

To what extent does the size affect the shear strength in the case of reinforced concrete beams higher than 3 meters without web reinforcement? Does the size effect in shear strength still remain unlimitedly? Can current design equations be extrapolated without problem? When we consider the likely size of concrete structures in the future, it is virtually impossible to come up with answers to these questions experimentally. It may be considered that any problems related to the size effect can be covered by including safety factors at the design stage. However, if the size effect cannot be evaluated correctly, the safety margin may prove inadequate as concrete structures go on increasing in size.

An analytical approach, rather than an experimental method, is strongly desired. Among the several possible approaches, fracture mechanics of concrete is considered to be the most promising way to carry out size effect analysis. Based on the fictitious crack model, which was originally proposed by Hillerborg [7], the authors have carried out size effect analysis for the shear strength of reinforced concrete beams. In this analysis, nonlinear rod elements representing the concrete's fracture properties are incorporated along the fictitious crack surface. According to the analytical results, it has been found that the size effect in shear strength rapidly disappears in huge reinforced concrete beams higher than 3 meters.

2. APPLICATION OF FRACTURE MECHANICS

2.1 Modeling the Crack

In usual finite element analysis to investigate the formation of cracks, cracking is normally judged based on the strength criterion. However, as a result of detailed investigations of crack formation, it has been demonstrated that the initiation of microcracks in the fracture process zone in front of a crack tip and the process of growth into a macroscopic crack must be modeled adequately and incorporated into the analysis. This means that the tension softening behavior and the fracture energy of concrete should be considered in the analysis.

The modeling of cracks in fracture mechanics takes two major forms: *the fictitious crack model* and *the crack band model.* In *the fictitious crack model*, the sequence of crack formation is represented by a local and macroscopic fictitious crack. The location of the fictitious crack is predetermined in the analysis. In *the crack band model*, the location of the crack does not need to be predetermined. During the crack formation process, the tension softening behavior and the fracture energy of the concrete are considered.

These two models have their own characteristics. *The fictitious crack model* treats the crack as a single discontinuity surface. Although this concept is quite clear, pre-processing is required to suitably determine the location of the fictitious crack. On the other hand, in *the crack band model*, the crack is assumed to form uniformly within the element. In this model, the location of the crack does not need to be predetermined, but the relationship between the localized volume of concrete in which cracking takes place and the fracture energy of the concrete must be considered systematically throughout the concrete structure in question.

In this research, *the fictitious crack model* was adopted. Although *the fictitious crack model* assumes that the actual crack formation process is very simple, the concept is clear and can easily be incorporated into the analysis.

2.2 Fictitious Crack Model

The fictitious crack model was originally proposed by Hillerborg [7]. The sequence of crack formation from the initiation of microcracks in concrete under tension through growth to development into major macroscopic cracks is modeled according to tension softening behavior. The tension softening behavior means that, once the tensile stress reaches the tensile strength of the concrete, the stress decreases as the fictitious crack increases in width. This behavior is represented by a tension softening curve. The area enclosed by the tension softening curve corresponds to the fracture energy of the concrete (Fig. 1). The fracture energy is defined as the energy required to create a fully cracked unit surface of concrete across which the tensile stress cannot be transferred (Eq. (1)).

$$G_F = \int_0^{w_o} \sigma \, dw \tag{1}$$

2.3 Use of Nonlinear Rod Element

In applying *the fictitious crack model*, the relationship between stress and crack width is generally utilized. For example, in the analytical method described by JCI research committee on fracture mechanics [8], two nodes are provided along the location of the fictitious crack and secant stiffness

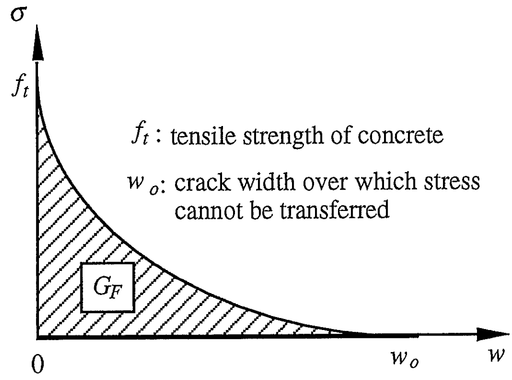

Fig. 1 Tension Softening Curve and Fracture Energy

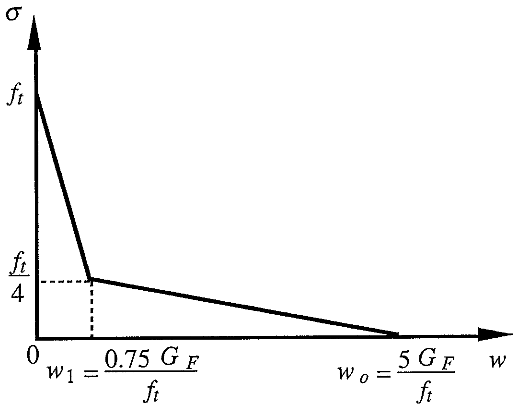

Fig. 2 One-Fourth Model

analysis is carried out using the location of the crack tip as the input data. However, a more general formulation is convenient for normal incremental finite element analysis.

In this analysis, a nonlinear rod element representing the tension softening behavior and the fracture energy of the concrete is inserted between two nodes placed at the location of the fictitious crack [9]. Using this rod element, it is possible to carry out normal incremental analysis. Furthermore, this analytical method can be extended to the case where a flexural crack and a shear crack coexist.

The tension softening curve has been obtained experimentally by various methods [10]. There are also various proposals for numerical models of the tension softening curve. In this analysis, the one-fourth bilinear model (Fig. 2) is adopted because it is widely accepted as the standard tension softening model.

Since the crack width w in the fictitious crack model can be converted into a strain ($\varepsilon = w/l$) by means of the length of the rod element l, the stress-crack width relationship can be transformed into a stress-strain relationship as follows:

(1) $0 \leq \varepsilon < \varepsilon_p$

$$\sigma = E_R \cdot \varepsilon \tag{2}$$

$$E_t = \frac{d\sigma}{d\varepsilon} = E_R \tag{3}$$

(2) $\varepsilon_p \leq \varepsilon < \varepsilon_1$

$$\sigma = f_t - \frac{0.75 f_t (\varepsilon - \varepsilon_p)}{\varepsilon_1 - \varepsilon_p} \tag{4}$$

$$E_t = \frac{d\sigma}{d\varepsilon} = -\frac{0.75 f_t}{\varepsilon_1 - \varepsilon_p} \tag{5}$$

(3) $\varepsilon_1 \leq \varepsilon < \varepsilon_o$

$$\sigma = 0.25 f_t - \frac{0.25 f_t (\varepsilon - \varepsilon_1)}{\varepsilon_o - \varepsilon_1} \tag{6}$$

$$E_t = \frac{d\sigma}{d\varepsilon} = -\frac{0.25 f_t}{\varepsilon_o - \varepsilon_1} \tag{7}$$

(4) $\varepsilon_o \leq \varepsilon$

$$\sigma = E_t = 0 \tag{8}$$

where, $\varepsilon_1 = \dfrac{0.75\, G_F}{f_t \cdot l}$, $\varepsilon_o = \dfrac{5\, G_F}{f_t \cdot l}$

The length l of the rod element is assumed to be unity (l=1) in the analysis (Fig. 3). In the elastic region before the tensile strength is exceeded ($\sigma < f_t$, $\varepsilon < \varepsilon_p$), no crack is initiated. In this region, to restrain elongation of the rod element (corresponding to the crack width), an extremely high stiffness is deliberately set for the rod element ($E_R = 100\, E_c$; E_c is the elastic modulus of the concrete).

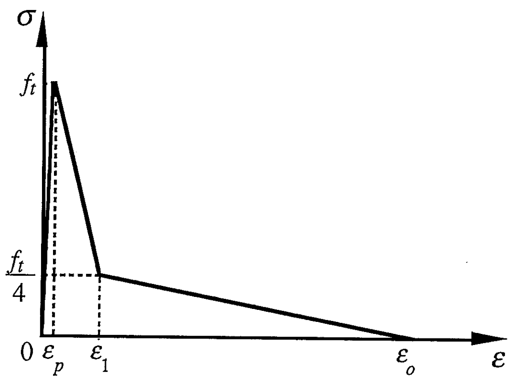

Fig. 3 Stress-Strain Relationship of a Rod Element

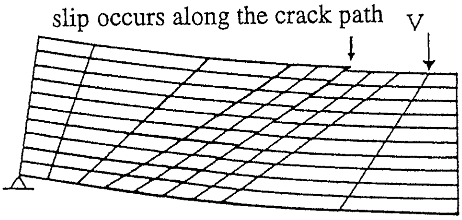

(a) only rod elements perpendicular to the crack path are provided

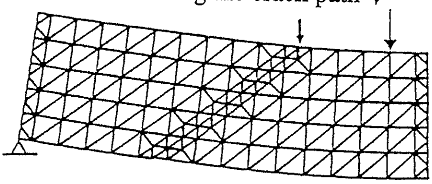

(b) rod elements perpendicular and parallel to the crack path are provided

Fig. 4 The Occurrence of Slip along the Fictitious Crack Path and its Prevention

Numerical analysis is executed by incorporating the tangential stiffness of this rod element into the total stiffness matrix.

2.4 Application of Orthogonal Rod Elements

A shear crack which causes diagonal tension failure is chosen as the subject of this research. Although a shear crack is supposed to have Mode II fracture properties and to differ from a flexural crack with Mode I fracture properties, it has been reported that shear cracks can be treated as Mode I cracks if the location is properly chosen [11]. This is because even shear cracks cannot slide relative to each other without exhibiting any opening. Therefore, in this analysis the fracture properties of the shear crack are assumed to be equal to those of a flexural crack.

According to analytical results with only perpendicular rod elements along the predetermined crack path, slip occurs along the assumed shear crack path from the very beginning of loading (Fig. 4(a)). The deformation shape shown in Fig. 4 corresponds to the first loading increment in the analysis and the applied shear force is less than 10% of the ultimate shear capacity. To make the situation clearer, the nodal displacements in Fig. 4 are intentionally amplified.

Because shear stiffness along the crack surface is completely neglected, slip along the crack path occurs as shown in Fig. 4(a). To prevent slip occurring as soon as the loading begins, the stiffness must be provided parallel to the crack direction as well as in the perpendicular direction.

This stiffness parallel to the crack direction should reflect the fracture property of concrete

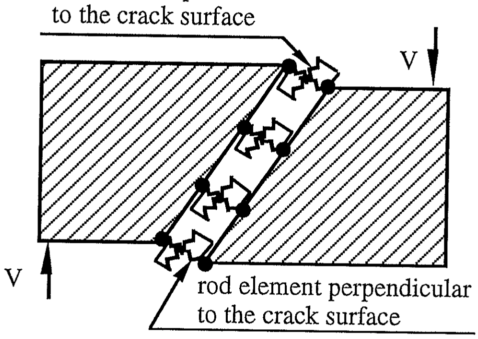

Fig. 5 Schematic Diagram of Orthogonal Rod Elements along the Fictitious Crack Surface

corresponding to the slip. At present, however, experimental information regarding slip failure is quite insufficient. In this analysis, therefore, another rod element parallel to the crack direction is placed in addition to the perpendicular rod element. The stiffness of this parallel rod element is assumed to be equal to the elastic shear modulus of the concrete before crack opening and is assumed to become completely zero after crack opening. The aim here is to model the stiffness as simply as possible. When experimental knowledge on Mode II cracking has been accumulated and the behavior is fully formulated, this simple analytical model can be replaced by a more accurate one.

After all, along the assumed shear crack path, perpendicular and also parallel rod elements are placed (Fig. 5). By making use of these orthogonal rod elements along the shear crack path, slip along the crack path in the early stages of loading can be completely prevented (Fig. 4(b)).

3. OUTLINE OF NUMERICAL CALCULATION

3.1 Analytical Procedure

The reinforced concrete beams chosen as the subject of this analysis have no shear reinforcement. In the analysis, the beams are assumed to be simply supported and subjected to two-point concentrated loading. Taking advantage of symmetry with respect to the center line, only half of the beam is analyzed. In the finite element analysis, all concrete elements except rod elements on the crack surface are assumed to be linear elastic and are modeled by a three-node triangular element. Longitudinal reinforcing bars are assumed to be elasto-plastic and are represented by a two-node truss element. Concrete nonlinearity is considered only in the rod elements. Incremental analysis using enforced displacement at the loading point as an input is executed. The Newton-Raphson method is used to update the tangential stiffness for the rod elements at every iteration.

3.2 Unloading and Reloading Paths in the Softening Curve

In reinforced concrete beams which exhibit diagonal tension failure when subjected to shear force, one large diagonal crack is observed at failure. Actually, in addition to this large diagonal crack which causes shear failure, a number of flexural cracks also occur in the beam. Therefore, to make the analysis more realistic, we have to consider an analytical model in which a shear crack and flexural cracks coexist.

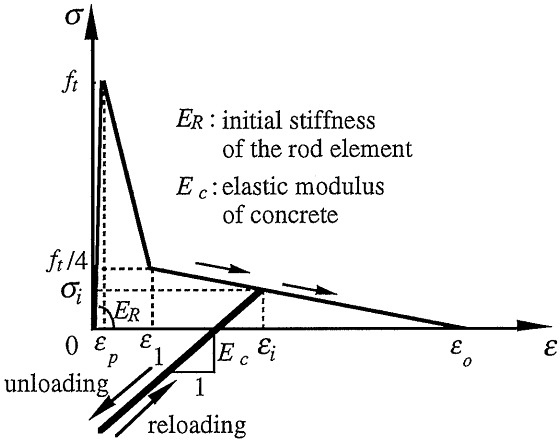

Fig. 6 Unloading and Reloading Paths in the Tension Softening Model

Although it is not impossible to place multiple fictitious cracks in the analytical model, the opening and closing behavior of the cracks has to be represented analytically. For example, the analysis has to model a situation where, although the opening of a flexural crack precedes the shear crack, the width of the flexural crack decreases with opening and propagation of the shear crack. To represent such opening and closing behavior of cracks, unloading and reloading paths must be formulated in the softening model of the concrete. Figure 6 shows the unloading and reloading paths adopted in this analysis. The tangential stiffness for unloading and reloading is assumed to be equal to the elastic stiffness of the concrete. Therefore, if the stress and strain at the unloading point are σ_i and ε_i, respectively, the stress-strain relationship in the unloading and reloading paths can be written as follows:

$$\sigma = \sigma_i + E_c(\varepsilon - \varepsilon_i) \tag{9}$$

$$E_t = \frac{d\sigma}{d\varepsilon} = E_c \tag{10}$$

4. NUMERICAL ANALYSIS FOR SHEAR STRENGTH

4.1 Basic Procedure

The most important point in applying *the fictitious crack model* is to determine the location of the crack adequately. The location of actual cracks varies remarkably depending on various factors such as loading conditions (distributed load or concentrated load), support conditions, bond characteristics of the longitudinal bars, degree of anchorage, concrete strength, and so on. Ultimately, a non-reproducible crack will cause experimental scatter in the shear strength. Although it is very hard to predict the location of cracks accurately, it is not very difficult to roughly evaluate a range for the location, the inclination angle, and the crack shape if experimental results are used for reference.

We determine the location and inclination angle of the shear crack as follows. Within the roughly evaluated range, the location and inclination angle are varied. The location and inclination angle at

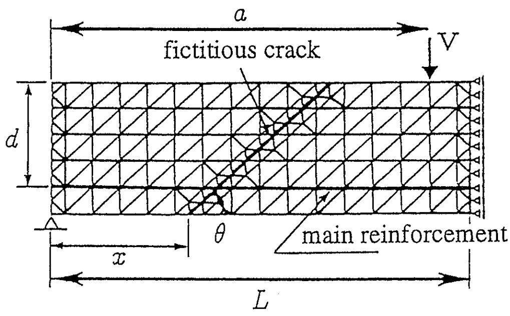

Fig. 7 The Mesh Discretization of Finite Element Analysis

which the shear resistance is a minimum are selected. The shape of the shear crack is basically assumed to be a single straight line. However, to simulate actual behavior more closely, i.e. the shear crack becoming flatter when it approaches the loading point, a bilinear straight line model for the shear crack is also examined. Furthermore, to make the analysis more realistic in the bilinear shear crack model, a flexural crack is also taken into account according to **3.2**. In this case, the location of the flexural crack is assumed to be at the span center and the crack surface is considered to be perpendicular to the beam axis. The shape of this flexural crack is fixed throughout the analysis.

4.2 Analytical Result using Single Straight Line Shear Crack

The finite element mesh discretization used in the analysis is shown in Fig. 7. The shear span - effective depth ratio, a/d, is fixed at 3.0. The width of the beam is 10 *cm*, and the height and effective depth of the beam are 12.5 *cm* and 10 *cm*, respectively. The reinforcement ratio is set to 2.0 %. The tensile strength, Young's modulus, and fracture energy of the concrete are 3.0 *MPa*, 0.3×10^5 *MPa*, and 100 *N/m*, respectively. The yield strength and Young's modulus of the reinforcing bars are 400 *MPa* and 2.0×10^5 *MPa*, respectively. These values are not changed throughout the analysis. The dimensions of the reinforced concrete beams, the diagonal crack parameters, and the results obtained are shown in Table 1.

Table 1 Dimensions of Beams, Parameters of Diagonal Cracks, and Analytical Results

$\theta = 40$ degrees		$x/d = 1.0$	
x/d	shear strength v_c *(MPa)*	θ (degrees)	shear strength v_c *(MPa)*
0.50	1.78	35	1.98
0.80	1.75	38	1.70
1.00	1.62	40	1.62
1.30	1.80	43	1.86
1.50	2.18	45	2.54

$b_w = 10\ cm$, $h = 12.5\ cm$, $d = 10\ cm$, $f_t = 3.0\ MPa$, $G_F = 100\ N/m$
$E_C = 0.3\text{x}10^5 MPa$, $\nu_C = 0.2$, $\rho_w = 2.0\ \%$, $f_y = 400\ MPa$
$E_S = 2.0\ \text{x}10^5 MPa$

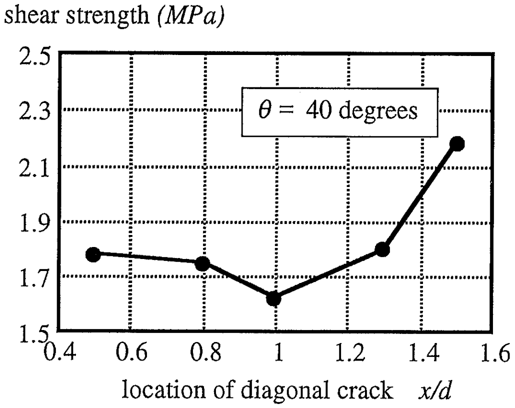

(a) change in shear strength with location of diagonal crack ($\theta = 40$ degrees)

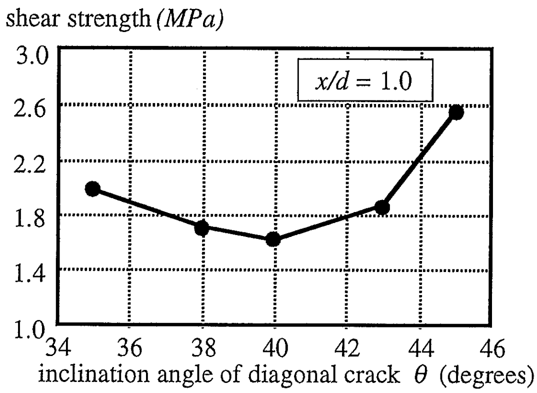

(b) change in shear strength with inclination angle of diagonal crack ($x/d = 1.0$)

Fig. 8 Change in Shear Strength with Assumptions about the Diagonal Crack

When modeling a diagonal crack by a single straight line, the parameters in the analysis are only the location and inclination angle of the assumed diagonal crack. The location of the crack can be represented by the distance from the support point to the point where the crack intersects the lower surface of the beam. The ratio of this distance x to the effective depth d (x/d) is varied from 0.5 to 1.5. As for the inclination angle of the assumed crack, the angle between the crack and the beam axis, θ, is varied from 35 to 45 degrees.

The variation in beam shear strength obtained from this analysis is shown in Fig. 8 (a) and (b). According to Fig. 8, it can be seen that the case of $x/d = 1.0$ and $\theta = 40$ degrees gives the minimum shear strength, v_c.

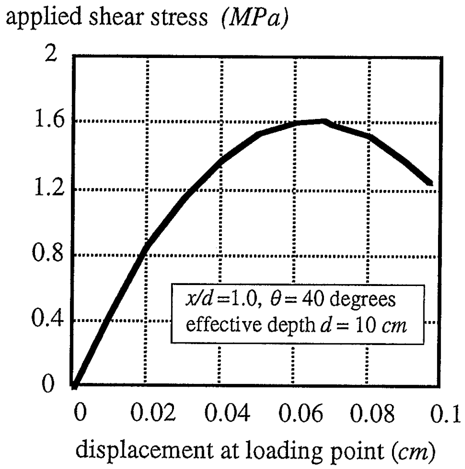

Fig. 9 Relationship between Applied Shear Stress and Displacement

Figure 9 shows the relationship between applied shear stress (= the nominal shear stress = $V/(b_w\ d)$) and displacement of the loading point for the case of $x/d = 1.0$ and $\theta = 40$ degrees. In this case, it is found that a stable softening path is followed in the post peak region because of the relatively small effective depth; i.e. 10 *cm*.

The nominal shear stress corresponding to the ultimate flexural capacity of the beam selected for parametric study is 2.28 *MPa*. The ultimate flexural capacity is obtained from a calculation based on the assumption of an equivalent stress block. Thus, the failure mode of beams implied by this analysis is shear failure prior to yielding of the longitudinal bars, except in the case of $x/d = 1.0$ and $\theta = 45$ degrees.

Although obtained shear strength for $x/d = 1.0$ and $\theta = 40$ degrees is 1.62 *MPa*, the value predicted by the macroscopic shear strength equation (Eq. (11)) is 1.48 *MPa*. The numerical analysis thus gives a slightly greater shear strength (= 1.09 times) than the macroscopic shear strength equation. This is due to certain simplifications in the analysis, such as taking only the shear crack into account and modeling it as a single straight line. However, it is worth pointing out that the result is not that far from the prediction by the macroscopic equation. Although the analytical results presented here are obtained from a simplified procedure in which material nonlinearity is taken into account only on the assumed crack surface, this analytical procedure is applicable to predictions of diagonal tension failure in which the initiation and propagation of one predominant diagonal crack control the failure of the whole structure.

4.3 Analytical Result using Bilinear Diagonal Shear Crack along with Flexural Crack

As described, a slightly greater shear strength than predicted by the macroscopic equation is obtained when a single straight line crack is assumed. It is also known that an actual shear crack becomes curved and flatter as it propagates into the flexural compression zone of a beam. Thus, to make the analytical procedure more realistic, a bilinear crack is now adopted as the assumed crack. Furthermore, for the same reasons, a flexural crack at the span center is also added.

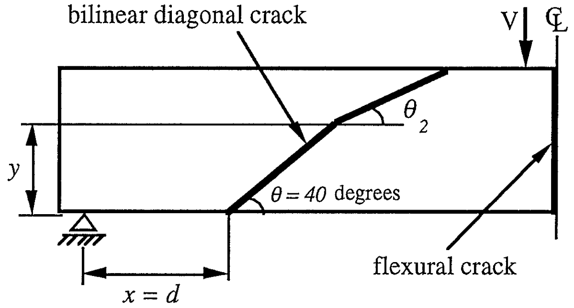

Fig. 10 Model of Bilinear Diagonal Crack

Table 2 Parameters of Diagonal Cracks and Analytical Results

$x/d = 1.0$, $\theta = 40$ degrees			
$\theta_2 = 30$ degrees		$y/d = 0.7$	
y/d	shear strength v_c (MPa)	θ_2 (degrees)	shear strength v_c (MPa)
0.5	1.43	20	1.40
0.6	1.40	25	1.38
0.7	1.37	30	1.37
0.8	1.39	35	1.38
0.9	1.41	40	1.39

As shown in Fig. 10, for the straight portion from the lower surface of the beam the assumption of $x/d = 1.0$ and $\theta = 40$ degrees is applied. However, for the flexural compression zone of the beam above this straight portion, another straight line is adopted. The parameters for this second straight line are the initiation point of the line (as represented by the height y from the lower surface of the beam) and the inclination angle of the line θ_2. The initiation point of the second line, y, is varied from 0.5 d to 0.9 d. The inclination angle, θ_2, is also varied from 20 to 40 degrees.

The results are shown in Table 2 and Fig. 11. These results show that an initiation point of 0.7 d and an inclination angle of 30 degrees for the second straight line give the minimum shear strength. The shear strength with these values is 1.37 *MPa*. The shear strength is 15 % lower in this analysis than in the case of a single straight line crack and no flexural crack. Since the shear strength is now almost 93 % of the value predicted by the macroscopic equation (1.48 *MPa*), the result is closer to the average of the macroscopic equation.

In conclusion, the accuracy of the shear strength prediction can be improved by adopting more realistic assumptions for the location, inclination angle, and shape of the fictitious crack and by using both a shear crack and a flexural crack. Figure 12 shows the opening and closing behavior of flexural and shear cracks.

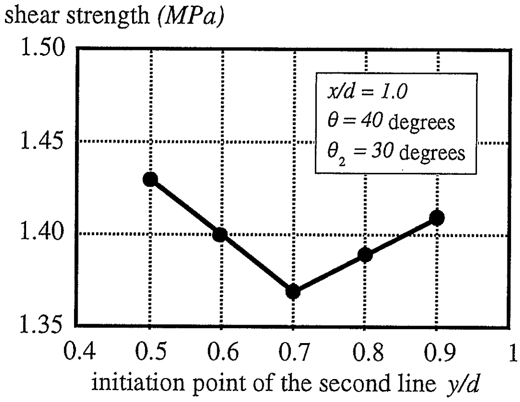

(a) change in shear strength with initiation point of the second line

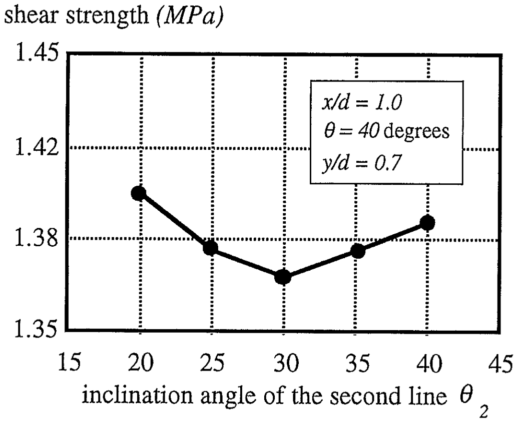

(b) change of shear strength with inclination angle of the second line

Fig. 11 Change in Shear Strength with Assumptions about the Diagonal Crack

The analytical nodal displacements are intentionally amplified in Fig. 12 to make crack opening and closing behavior more visible. The applied shear force corresponds to about 50 % and 95 % of the maximum shear capacity (i.e. the peak resistance obtained from analysis), respectively. Figure 12 also makes clear that, at the shear force corresponding to 50% of the peak resistance, only the flexural crack opens and the shear crack is closed, while at the shear force corresponding to the peak resistance, the shear crack develops and propagates but the flexural crack width becomes relatively smaller.

5. SIZE EFFECT IN SHEAR STRENGTH

The numerical analysis carried out in Chapter **4** gives a rough means of determining the location, inclination angle, and shape of a diagonal crack. Thus, based on this information about diagonal

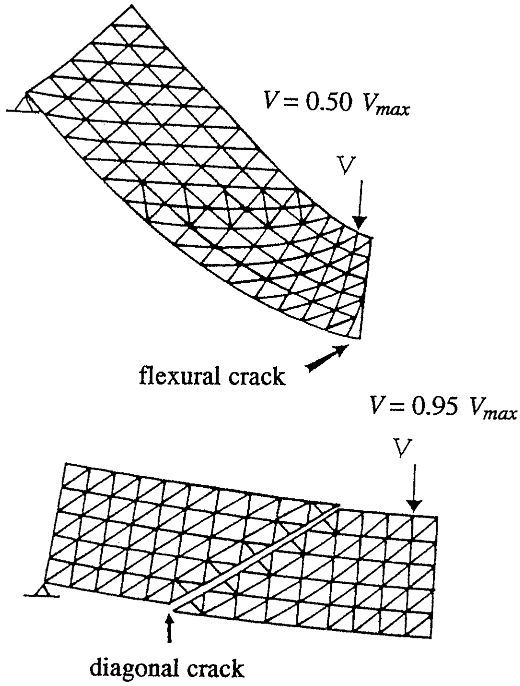

Fig. 12 Opening and Closing Behavior of Cracks
Depending on Shear Force

cracking, the size effect in shear strength is now evaluated numerically. The resulting size effect will be compared with the shear strength equations stipulated in the JSCE Standard Specifications and CEB-FIP Model Code 1990.

The shape and dimensions of the reinforced concrete beams chosen as the subject of this numerical study are shown in Table 3 along with the calculated results. These beams are geometrically similar in two dimensions. The size of the finite elements is also increased in a geometrically similar manner. The height of the beam h is varied from 10 cm to 10 m. Figure 13 is a comparison of the analytical results with the shear strength equations stipulated in the JSCE Standard Specifications (Eq. (11)) and CEB-FIP Model Code 1990 (Eq. (12)).

$$v_{c.JSCE} = 0.20\ (100\rho_w \cdot f_c')^{1/3}\ d^{-1/4} \tag{11}$$

$$v_{c.CEB} = 0.15\ (100\rho_w \cdot f_c')^{1/3}\ (1 + \sqrt{0.2/d}\ ) \tag{12}$$

where, in these equations, the shear strength, v_c, and the compressive strength of concrete, f_c', are in MPa units and the effective depth, d, is in m units. Since the compressive strength of concrete, f_c', is required in these equations, it is calculated from Eq. (13) using the tensile strength, f_t.

Table 3 Dimensions of Beams and Analytical Results

No.	h (cm)	d (cm)	a (cm)	$v_{c.cal}$ (MPa)	$v_{c.\ JSCE}$ (MPa)	$v_{c.\ CEB}$ (MPa)
1	10	9	27	1.401	1.523	1.559
2	50	45	135	0.940	1.019	1.043
3	100	90	270	0.837	0.857	0.921
4	300	270	810	0.788	0.651	0.796
5	500	450	1350	0.761	0.573	0.758
6	1000	900	2700	0.725	0.482	0.719

$b_w = 10\ cm,\ f_t = 3.0\ MPa,\ G_F = 100\ N/m,\ E_C = 0.3\text{x}10^5\ MPa$
$f_c' = 37\ MPa,\ \rho_w = 2.0\ \%,\ f_y = 400\ MPa,\ E_S = 2.0\ \text{x}10^5\ MPa$
$\theta = 40$ degrees, $\theta_2 = 30$ degrees, $x/d = 1.0$, $y/d = 0.7$

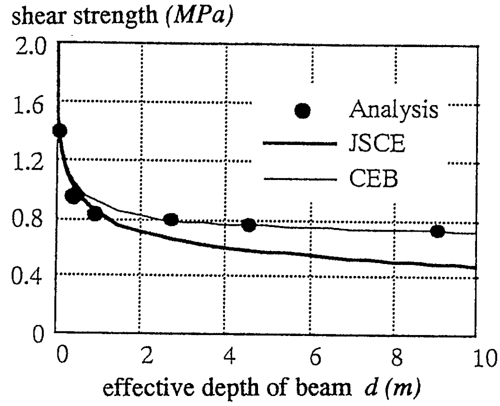

Fig. 13 Size Effect in Shear Strength

$$f_t = 0.27\ (f_c')^{2/3} : MPa \qquad \left(f_t = 0.58\ (f_c')^{2/3} : kgf/cm^2\right) \tag{13}$$

As shown in Fig. 13, the analytical results agree very well with the JSCE equation in the region of effective depth d less than 1 m and agree with the CEB equation in the region where d is more than 1 m. In Eq. (11), the shear strength decreases monotonically with increasing effective depth. On the other hand, in Eq. (12), the shear strength converges to a constant value. This is the major difference between these two design equations.

Data to experimentally support the shear strength equation stipulated in the JSCE Standard Specifications are limited to effective depths up to 3 m. Where the effective depth, d, is more than 3 m, there is no experimental support for the equation. As far as the analytical results obtained here are

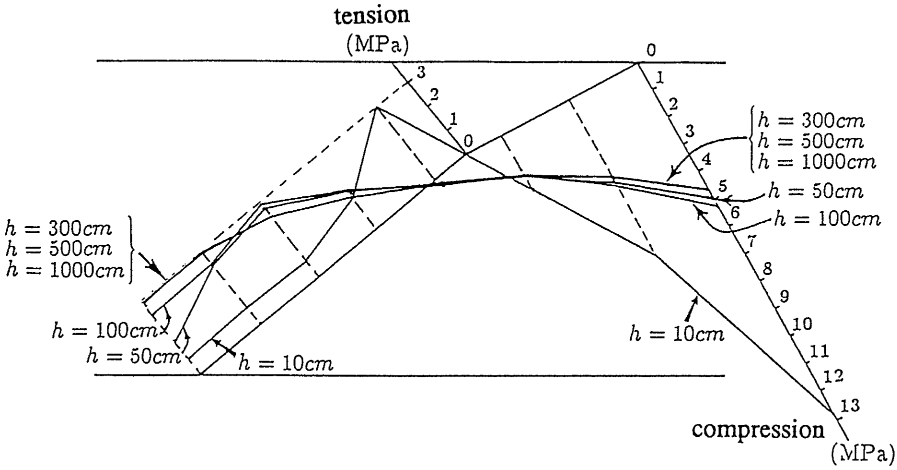

Fig. 14 Change in Stress Distribution among Rod Elements along the Diagonal Crack Surface Depending on Height of Beam

concerned, it can be concluded that the application of the JSCE's shear strength equation to huge reinforced concrete beams with an effective depth of more than 3 m gives a conservative result and the JSCE's shear strength equation virtually underestimates the actual shear strength.

Figure 14 shows the obtained stress distribution in perpendicular rod elements at peak resistance along the assumed diagonal crack. To make the comparison easy, the location of the rod elements is normalized by the height of the beam. According to Fig. 14, within the region of the effective depth up to 1 m, the rod element in which the stress reaches the tensile strength of the concrete is located from the third to the fifth layer above the lower surface of the beam, and rod elements below this rod element are in the tension softening region. However, the stress distribution among perpendicular rod elements in reinforced concrete beams with an effective depth greater than 3 m is almost similar; when the stress in the lowest rod element reaches the tensile strength of the concrete, the beam exhibits peak resistance. This suggests the disappearance of the size effect.

In the diagonal tension failure of reinforced concrete beams without web reinforcement, as well as in the flexural failure of plain concrete beams, sudden and brittle failure occurs when the stored strain energy in the beam at the peak exceeds the energy required to cause shear failure. In this case, the decrease in shear strength due to the increase in beam size does not become significant.

6. CONCLUSIONS

In this research work, the size effect in the shear strength of reinforced concrete beams without web reinforcement has been numerically evaluated using an approach based on fracture mechanics of concrete. The conclusions reached can be summarized as follows:

(1) By providing rod elements parallel to the fictitious crack direction in addition to rod elements

perpendicular to the fictitious crack direction incorporating the fracture properties of the concrete, slip along the fictitious crack can be prevented as loading begins.

(2) Changing the location and inclination angle of the diagonal crack allows an analytical model corresponding to the minimum shear resistance to be determined. Furthermore, assuming the coexistence of a flexural crack and a diagonal crack makes the analysis more realistic; in this case, the diagonal crack is changed from a single straight line to a bilinear line.

(3) A parametric study confirms that the coexistence of a flexural crack and a diagonal crack and the bilinear diagonal crack model give a more realistic analytical result.

(4) On the basis of this analytical model, a parametric analysis for geometrically similar beams for size effect shows that when the height of the beam is less than 1 *m*, the obtained shear strength agrees well with predictions by the design equation stipulated in the JSCE Standard Specifications. However, for huge beams of height more than 3 *m*, the size effect predicted by the JSCE equation disappears and the size effect is more like that predicted by the design equation in the CEB-FIP Model Code.

(5) From an investigation of stress distribution in the perpendicular rod elements at peak resistance, huge beams of height more than 3 *m* are observed to fail in shear before tension softening of concrete along the diagonal crack occurs.

(6) Considering these findings, it can be concluded that the size effect in the shear strength of reinforced concrete beams without web reinforcement gradually disappears as beam height increases. Since the design equation stipulated in the JSCE Standard Specifications has sufficient experimental backing, the accuracy of its predictions is good within the range of the experimental data. However, the design equation may underestimate the shear strength when the height of a beam is outside the range of existing experimental data.

In this research work, the problem investigated was restricted to reinforced concrete beams subjected to concentrated loading. However, it is also possible to extend the analysis to more realistic problems, such as reinforced concrete beams subjected to uniform loading or axial loading, by changing the analytical boundary conditions. Extension of the analysis to such problems is planned as future work.

ACKNOWLEDGEMENT

The authors are grateful to Mr. Shigenori Hidaka (graduate student at Nagoya University) for drawing the figures. The cooperation of Mr. Hidaka is greatly appreciated.

REFERENCES

[1] Okamura, H., & Higai, T.: Proposed Design Equation for Shear Strength of Reinforced Concrete Beams without Web Reinforcement, Proc. of JSCE, No. 300, pp. 131-141, 1980

[2] Iguro, M., Shioya, T., Nojiri, Y., & Akiyama, H.: Experimental Study on Shear Strength of Large-sized Reinforced Concrete Beams Subjected to Uniform Loading, Proc. of JSCE, No. 348, V-1, pp. 175-184, 1984 (in Japanese)

[3] Niwa, J., Yamada, K., Yokozawa, K., & Okamura, H.: Revaluation of the Equation for Shear Strength of Reinforced Concrete Beams without Web Reinforcement, Proc. of JSCE, No. 372, V-5, pp. 167-176, 1986 (in Japanese)

[4] ACI: Building Code Requirements for Reinforced Concrete (ACI 318-89), 353 pp., 1989

[5] CEB: CEB-FIP Model Code for Concrete Structures, 348 pp., 1978
[6] CEB: CEB-FIP Model Code 1990, Bulletin d'Information, No. 213/214, 437 pp., 1993
[7] Hillerborg, A. et al.: Analysis of Crack Formation and Crack Growth in Concrete by Means of Fracture Mechanics and Finite Element, Cement and Concrete Research, Vol. 6, No. 6, pp. 773-782, 1976
[8] JCI Research Committee on Fracture Mechanics of Concrete: Committee Report, Proc. of the Colloquium on Fracture Mechanics of Concrete Structures, 176 pp., 1990 (in Japanese)
[9] Niwa, J.: Size Effect Analysis for Flexural Strength of Concrete Beams Using Nonlinear Rod Element, Proc. of JCI, Vol. 15, No. 2, pp. 75-80, 1993 (in Japanese)
[10] Uchida, Y., Rokugo, K., & Koyanagi, W.: Estimation and Measurement of Tension Softening Curve of Concrete Based on Flexural Tests, Proc. of JSCE, No. 426, V-14, pp. 203-212, 1991 (in Japanese)
[11] Blaauwendraad, J., & Wang, Q.B.: Systematic Fracture Mechanics Study of Shear Failure in Beams under Distributed Load, IABSE Colloquium on Structural Concrete, IABSE Report, Vol. 62, pp. 637-642, 1991